Applied Physics Letters

Experimental validation of deep-subwavelength diffusion by acoustic metadiffusers

Cite as: Appl. Phys. Lett. **115**, 081901 (2019); https://doi.org/10.1063/1.5114877
Submitted: 12 June 2019 . Accepted: 01 August 2019 . Published Online: 20 August 2019

E. Ballestero, N. Jiménez, J.-P. Groby, S. Dance, H. Aygun, and V. Romero-García

Applied Physics Letters ARTICLE scitation.org/journal/apl

Experimental validation of deep-subwavelength diffusion by acoustic metadiffusers

Cite as: Appl. Phys. Lett. **115**, 081901 (2019); doi: 10.1063/1.5114877
Submitted: 12 June 2019 · Accepted: 1 August 2019 ·
Published Online: 20 August 2019

E. Ballestero,[1,a)] N. Jiménez,[2] J.-P. Groby,[3] S. Dance,[1] H. Aygun,[1] and V. Romero-García[3]

AFFILIATIONS

[1]The Acoustics Group, London South Bank University, 103 Borough Road, London SE1 0AA, United Kingdom
[2]Instituto de Instrumentación para Imagen Molecular, Consejo Superior de Investigaciones Científicas (CSIC), Universitat Politècnica de València, Camino de Vera s/n, 46022 València, Spain
[3]Laboratoire d'Acoustique de l'Université du Mans, LAUM - UMR CNRS 6613, Le Mans Université, Avenue Olivier Messiaen, 72085 LE MANS CEDEX 9, France

[a)]**Author to whom correspondence should be addressed:** balleste@lsbu.ac.uk/ballesteroeric@outlook.com

ABSTRACT

An acoustic metadiffuser is a subwavelength locally resonant surface relying on slow sound propagation. Its design consists of rigidly backed slotted panels, with each slit being loaded by an array of Helmholtz resonators. Due to the slow sound properties, the effective thickness of the panel can therefore be dramatically reduced when compared to traditional diffusers made of quarter-wavelength resonators. The aim of this work is to experimentally validate the concept of metadiffusers from the scattering measurements of a specific metadiffuser design, i.e., a quadratic residue metadiffuser. The experimental results reported herein are in close agreement with analytical and numerical predictions, therefore showing the potential of metadiffusers for controlling sound diffusion at very low frequencies.

Scattering of waves is one of the most analyzed phenomena in wave physics, and many applications using structures and surfaces that control the reflection of waves are exploited in several branches of science and technology. In acoustics, systems presenting a uniform scattering function, i.e., structures that reflect impinging waves in many different directions, have been largely developed since the pioneering work on acoustic diffusers by Schroeder in the 1970s.[1] These locally reacting surfaces spread reflected waves into all directions, reducing the strength of the undesired specular reflections and audible echoes, while sound energy is preserved in space. The spatially dependent reflectivity of a sound diffuser is generally tailored following numerical sequences with a uniform spatial Fourier transform of their reflection coefficient such as the Quadratic Residue (QR), Maximum Length (MLS), Primary Root (PR), or Index sequences.[2,3] Traditionally, these structures, also called Schroeder diffusers, are designed using rigidly backed slotted panels where each well acts as a quarter-wavelength resonator (QWR). Therefore, these phase-grating diffusers become thick and heavy structures when designed to manage low-frequency waves, e.g., the typical thickness of a quadratic residue diffuser (QRD) is half of the wavelength corresponding to the low cut-off frequency. In this way, their application is very limited in critical listening environments such as auditoria, professional broadcast and recording control rooms, recording studios, or conference rooms to control low-frequency sound.

Several approaches have been proposed in the past to overcome these limitations. Good folding strategies were proposed to minimize the unused space between slots.[4,5] Later, Hunecke *et al.*[6] proposed to close the quarter wavelength resonators (QWRs) by perforated or microperforated sheets,[2,7] adding inertia to the impedance of the wells in order to lower the resonance frequencies and hence lower the design frequency. Recently, sonic crystals (SCs) were used to construct volumetric acoustic diffusers.[8,9] In addition, optimized sound diffusers made of slotted panels incorporating two dimensional Helmholtz resonators (HRs) instead of QWRs are already commercialized.[10] By using HRs, the resonance frequency of each well can be downshifted, thus extending the diffusion bandwidth. This idea has recently been revisited by using metamaterials, allowing the design of metasurfaces presenting simultaneously efficient diffusion properties and subwavelength dimensions. In 2017, Zhu *et al.*[11] revisited the problem to design an ultrathin QRD using a planar array of HRs. The efficiency of this ultrathin QRD is focused on the low frequency range. Also in 2017, the concept of metadiffusers was proposed by Jiménez *et al.*[12] These sound diffusers are rigidly backed slotted panels based on slow-sound metamaterials, i.e., each slit is loaded by an array of Helmholtz resonators. In essence,

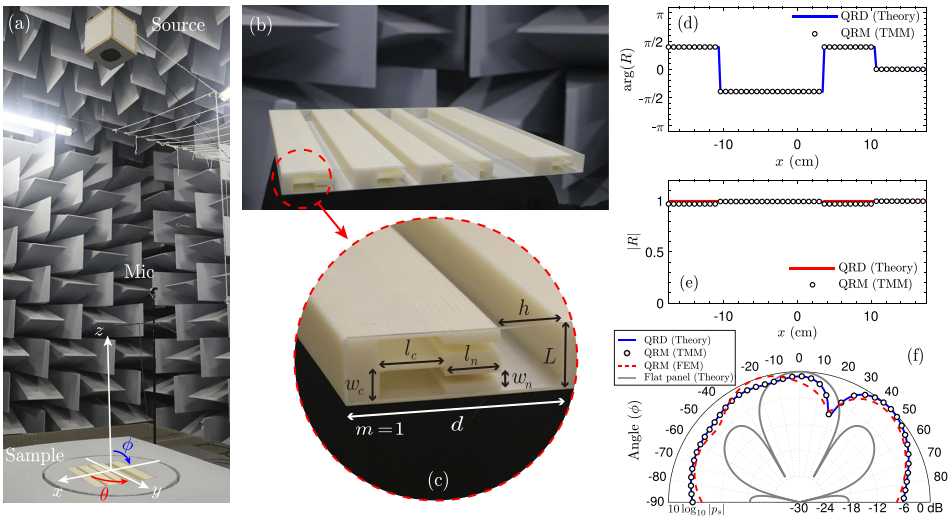

FIG. 1. (a) Experimental setup and coordinate system. (b) Photograph of the QRM. (c) Details of the first slit ($m = 1$) showing the definition of the geometrical parameters. (d) Phase and (e) magnitude of the spatially dependent reflection coefficient for an ideal QRD (continuous lines) and the tailored QRM (markers). (f) Far-field polar distribution at 2 kHz of an ideal QRD (continuous-blue), QRM obtained theoretically by TMM (circles) and numerically by FEM (dashed red), and a plane reference reflector with the same dimensions (thick-gray).

strong dispersion is introduced and the effective sound speed inside each slit is drastically reduced in the low frequency regime[13,14] due to the loading HRs. In this way, the quarter-wavelength resonance is shifted to the deep-subwavelength regime, and therefore, the effective thickness of the panel can be strongly reduced.[15–17] Various two-dimensional (2D) designs have been theoretically and numerically presented, showing a strong reduction of the thickness of the panel of about a twentieth and a tenth of the thickness of traditional designs. As an example, a design of an optimized broadband metadiffuser panel of 3 cm thickness working from 250 Hz to 2 kHz was presented,[12] i.e., the panel is then 24 times thinner than the low cut-off wavelength of the intended sequence.

An experimental validation of the concept of acoustic metadiffusers is reported in this work. A QR metadiffuser (QRM) has been 3D-printed, proving to scatter sound efficiently in one plane. The diffusion properties of the QRM were characterized experimentally in an anechoic chamber following the procedure outlined in ISO 17497-2:2012.[18] Note that the original design[12] was purely two-dimensional; however, in practice, the structure must be bounded and the final structure thus becomes finite in the three dimensional space. The experimental results of the QRM and a reference flat rigid reflector are compared with 3D numerical predictions of the finite structures using the Finite Element method (FEM) including thermoviscous losses. The experimental results reported herein are in close agreement with simulations and theory, therefore showing the potential of metadiffusers for controlling sound diffusion at the subwavelength scale.

The panel was manufactured using fused deposition modeling (FDM) techniques (Stratasys Fortus 450 MC), as shown in Figs. 1(a)–1(c). The squared panel, of $L = 2$ cm thickness and side $Md = 35$ cm, is composed of $M = 5$ slits, and each slit is loaded with 2 identical HRs. This QRM mimics the behavior of a classical QRD made of M wells and a total thickness of $L = 27.4$ cm designed for a low cut-off frequency of 500 Hz. Note that the design frequency is normally set as the lower frequency limit of the diffuser, but it is not necessarily the lowest frequency at which the surface produces more scattering than a plane surface: the ratio between the size of the panel and the wavelength must be accounted for.[19] In this work, the response was evaluated at 2000 Hz to avoid the strong diffractive regime of the finite panel due to the small lateral size. The spatially dependent reflection coefficient calculated from the QR sequence is given by $s_m = m^2 \bmod(M)$, where $\bmod(M)$ is the least non-negative remainder of the prime number M. For a classical QRD, the depth of the wells in the sequence is thus given by[19] $L_m = s_m \lambda_0 / 2M$, where λ_0 is the design wavelength. The dimensions of the slits and HRs of the QRM which mimic the reflection coefficient of the QRD are shown in the supplementary material. The magnitude and phase of the reflection coefficient along the x-direction of the ideal QRD and the QRM, as calculated by using the transfer matrix method (TMM),[12] are shown in Figs. 1(d) and 1(e). Here, the reflection coefficient is evaluated considering the viscothermal losses existing in both the QRD and the QRM.[20] Notice that the thickness of the QRM is reduced by a factor of 13 with respect to the classical QRD one, while both responses match.

The far-field pressure distribution at normal incidence, $p_s(\theta, \phi)$, of a reflecting rectangular surface with a spatially dependent reflection coefficient, $R(x, y)$, of size $2a$ and $2b$ in the x and y directions, respectively, can be calculated using the Fraunhofer integral[21]

$$p_s(\theta, \phi) = \int_{-a}^{a} \int_{-b}^{b} R(x, y) e^{ik(x \sin\phi \sin\theta + y \sin\phi \cos\theta)} \mathrm{d}x\mathrm{d}y, \qquad (1)$$

where θ and ϕ are the azimuthal and elevational angles, respectively. Figure 1(f) shows the far-field calculations in the x-varying plane at 2000 Hz for a QRD, the QRM, and a flat reference reflector of the same dimensions. Excellent agreement is observed between the polar responses obtained by the direct integration of Eq. (1) with the reflection coefficient profiles of the QRD and the QRM shown in Figs. 1(d) and 1(e) with the full-wave numerical solution of the QRD problem using FEM (see further details of the methods in the study by Jiménez *et al.*[12]). Note that viscothermal losses were accounted for in both cases.

An experimental procedure based on ISO 17497-2:2012[18] was developed here to determine the sound scattering properties of the metadiffusers. As such, measurements consisted in placing the physical sample (e.g., the QRM or the flat reference panel) at the center of a virtual concentric arc of evenly spaced microphone positions, all within an anechoic environment and keeping unwanted acoustical contributions from the measurement system as minimal as possible, as shown

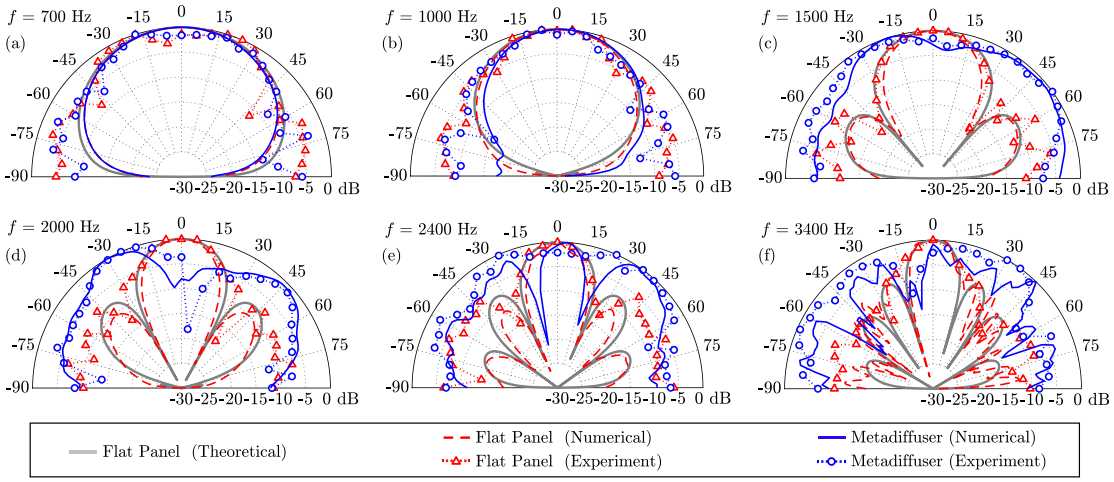

FIG. 2. Scattered field distribution, $p_s(90^\circ, \phi)$, for normal sound incidence at different frequencies obtained experimentally in the near-field (markers) and numerically for the QRM (blue) and the flat reference panel (red) in the far-field. Theoretical far-field pressure distributions for the flat panel are shown in thick-gray lines.

in Fig. 1(a). Microphone positions ranged from $\phi = 0^\circ$ to $\phi = 90^\circ$ around the surface with a spacing of 6° between each and along an arc radius of 1 m. The sample was placed on a rotating table, thus allowing a complete hemispherical characterization of the surface's scattering along the polar circle in the θ direction. Measurements were performed for normal incidence by locating the source 2.5 m away from the surface. The system was excited using a broadband Maximum Length Sequence (MLS) signal, and impulse responses (IRs) at each microphone position were obtained by deconvolution. Each IR was subtracted from the one obtained from the anechoic background and windowed to extract the scattered sound field.[18] Then, the polar distribution of the scattered field was obtained after Fourier transformation.

The experimental, analytical, and simulated scattered field distributions in the $\theta = 90^\circ$ cross section are shown in Fig. 2 for both the QRM and the flat reference panel. Analytical solutions of Eq. (1) for a finite rigid panel of dimensions $a = b = 35$ cm can be found in the literature.[21] Here, we show frequencies ranging from 700 Hz to 3.4 kHz. On the one hand, the simulated scattered field of the flat panel agrees with the analytical one (continuous-red and thick-gray, respectively). Slight deviations are observed at 2.4 kHz and 3.4 kHz, mainly caused by the finite thinness of the panel in the simulation. The measured scattered field of the flat panel (red triangles) also shows a strong agreement with the simulated and theoretical ones, except at grazing angles ($\phi > 60^\circ$) where higher scattering values are observed. This occurs because the weak reflected energy by the panel at the grazing angle is comparable to the spurious reflections of the anechoic chamber grid that covers the floor. However, this effect has a very low impact on the diffusion coefficient values, as we will see later. On the other hand, the measured scattered field values for the QRM (blue circles) are in close agreement with the far-field ones (continuous-blue) obtained through FEM simulations. Note that the dips observed in the simulations are smoothed in the experimental data, and the overall distribution shape is conserved. At low frequencies, e.g., 700 Hz, simulated curves for the flat panel and QRM illustrate the fact that the QRM behaves in a similar manner to that of the flat panel, showing the need of normalization to estimate the diffusion performance of the sample.

Ultimately, the directional diffusion coefficient[22] produced when the diffuser is radiated by a plane wave at the incident angle (θ', ϕ'), $\delta_{\theta',\phi'}$, can be estimated from the hemispherical distributions as

$$\delta_{\theta',\phi'} = \frac{\left[\int\int I_s(\theta,\phi)dS\right]^2 - \int\int I_s^2(\theta,\phi)dS}{\int\int I_s^2(\theta,\phi)dS}, \quad (2)$$

where $I_s(\theta,\phi) = |p_s(\theta,\phi)|^2$ is proportional to the scattered intensity. The integration is performed over a hemispherical surface ($-\pi/2 \le \phi \le \pi/2$ and $\theta = 2\pi$), where $dS = d\theta d\phi$. In this work, we analyze the case of a normal incident wave, i.e., $\theta' = 0$ and $\phi' = 0$. Therefore, $\delta_{\theta',\phi'} \equiv \delta_0$. This coefficient must be normalized to that of a plane reflector, δ_{flat}, to eliminate the effect of the finite size of the structure as $\delta_n = (\delta_0 - \delta_{\text{flat}})/(1 - \delta_{\text{flat}})$.

Figure 3(a) shows the frequency-dependent directional diffusion coefficients, δ_0, for the QRM and the flat panel. First, the experimental diffusion coefficient for the flat panel is in close agreement with the analytical one, and as expected, higher diffusion values are achieved in the low frequency regime due to the diffraction of the finite sample. The same phenomenon can be observed for the QRM (blue continuous) in this low frequency regime as it matches the values obtained for the flat panel. This is mainly due to the lack of any slit resonance within the metasurface and is thus illustrated by the normalized diffusion coefficient of the QRM taking values around zero. However, when approaching the frequency $f \approx 1000$ Hz, the dispersion in the slits progressively changes, and the impedance of each deep-subwavelength slit is hence modified. The complex reflection coefficient thus becomes spatially dependent, and following Eq. (1), the scattering distribution starts to be modified, resulting in higher values of the normalized diffusion coefficient δ_0. Eventually, the spatially dependent reflection coefficient matches the one of a QRD at $f = 1500$ Hz. At this frequency, the experimental diffusion coefficient takes a value of $\delta_0 = 0.783$, while the corresponding simulation is placed at a very close value of $\delta_0 = 0.786$. The normalized diffusion coefficient takes a value of $\delta_n = 0.708$ in the experiment and $\delta_n = 0.712$

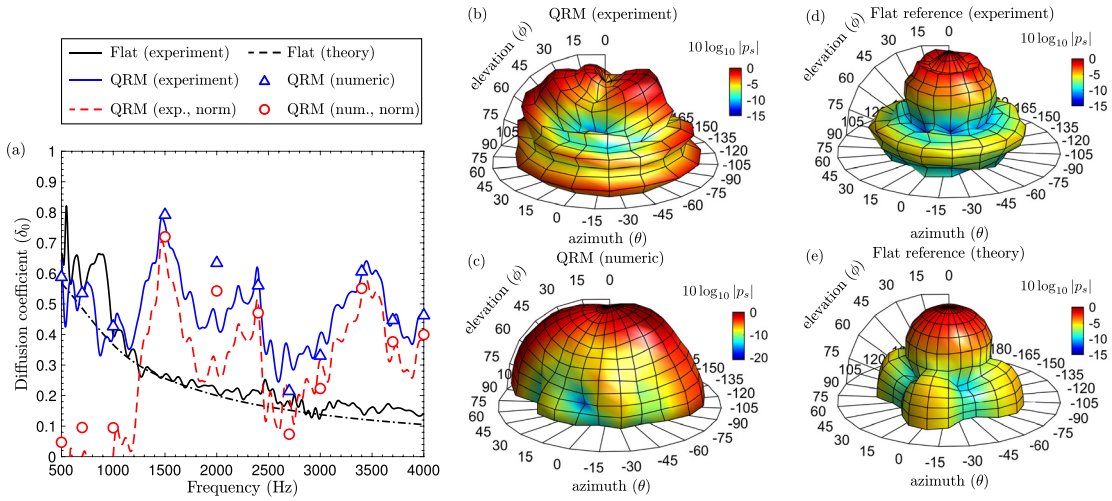

FIG. 3. (a) Diffusion coefficients of the QRM and a flat reference panel. Scattered field distribution, $p_s(\theta, \phi)$, for the QRM at 1500 Hz (b) measured experimentally and (c) by FEM simulations. [(d) and (e)] Corresponding scattered field distribution for the flat reference panel.

in the simulation, keeping these values in the range of those reported for classical QRDs.[19] Note that the normalized diffusion coefficient using 1D theory [see Fig. 1(f)] is very similar ($\delta_n = 0.69$). However, the latter 1D diffusion value must not be directly compared with the results in Fig. 3(a) as oblique and transversal modes along the y-direction are not included in the 1D theory. The presence of such modes will affect the impedance of the slits and will thus result in a change of the scattering properties of the surface. The experimental and simulated and theoretical scattering distributions at $f = 1500$ Hz at a distance of 1 m from the sample are shown in Figs. 3(b)–3(e). For the QRM, the waves are reflected evenly for the azimuthal plane, $\theta = \pm 90°$, corresponding to the cross section of the slits as $R(x, y)$ only shows variations in the x-direction. This is an expected behavior observed in any 1D phase grating diffuser and particularly useful to anisotropically control reflections in critical listening spaces.[19] In contrast, the flat panel mainly scatters waves in the specular direction. Both experimental and numerical scattering distributions agree with each other except grazing angles as explained above. Complementary 3D plots at other frequencies and animated videos illustrating the simulated behavior of the QRM and flat panel are available in the supplementary material.

We have experimentally demonstrated the efficiency of metadiffusers, i.e., deep-subwavelength metasurfaces with uniform scattering distribution in the subwavelength regime. The scattering distributions observed experimentally using 3D panels are in close agreement with simulated and measured ones and agree with the theoretical designs.[12] A remarkable high diffusion performance is demonstrated by the experimental normalized diffusion coefficient of $\delta_n > 0.7$ at 1500 Hz. The results demonstrate the possibility of metadiffusers to be applied in many practical situations where the classical solutions are limited due to the lack of space and structure weight. This includes applications ranging from opera pits[2] to aerospace applications.[23] This study allows us to push forth toward the situation-specific designs of optimized metadiffusers and to continue measuring their scattering characteristics in order to solidify the knowledge of such subwavelength metasurfaces.

See the supplementary material for more details of the calculations and animation of sound scattering by acoustic metadiffusers.

This article was based upon the work from COST Action DENORMS CA15125, supported by COST (European Cooperation in Science and Technology). This study was financed by London South Bank University, the Royal Opera House, Covent Garden, and the United Kingdom Acoustics Network (UKAN). The authors gratefully acknowledge the ANR-RGC METARoom (No. ANR-18-CE08-0021) project and the project HYPERMETA funded under the program Étoiles Montantes of the Région Pays de la Loire. N.J. acknowledges the financial support from Generalitat Valenciana through Grant No. APOSTD/2017/042.

REFERENCES

[1]M. R. Schroeder, J. Acoust. Soc. Am. **57**, 149 (1975).
[2]T. Cox and P. D'Antonio, Build. Acoust. **10**, 1 (2003).
[3]T. J. Cox and P. D'Antonio, *Acoustic Absorbers and Diffusers: Theory, Design and Application* (CRC Press, 2009), pp. 295–306.
[4]F. Mechel, Acta Acust. Acust. **81**, 379 (1995).
[5]J. Hargreaves and T. Cox, Proc. Inst. Acoust. **25**, 199 (2003).
[6]J. Hunecke, "Schallstreuung und Schallabsorption von Oberfl: Ahen aus mikroperforierten Streifen," Ph.D. thesis (University of Stuttgart, 1997).
[7]T. Wu, T. J. Cox, and Y. Lam, J. Acoust. Soc. Am. **110**, 3064 (2001).
[8]R. J. Hughes, J. A. Angus, T. J. Cox, O. Umnova, G. A. Gehring, M. Pogson, and D. M. Whittaker, J. Acoust. Soc. Am. **128**, 2847 (2010).
[9]J. Redondo, R. Picó, V. J. Sánchez-Morcillo, and W. Woszczyk, J. Acoust. Soc. Am. **134**, 4412 (2013).
[10]P. DAntonio, "Planar binary amplitude diffusor," US patent US55817992A (1998).
[11]Y. Zhu, X. Fan, B. Liang, J. Cheng, and Y. Jing, Phys. Rev. X **7**, 021034 (2017).
[12]N. Jiménez, T. J. Cox, V. Romero-García, and J.-P. Groby, Sci. Rep. **7**, 5389 (2017).

[13]J.-P. Groby, W. Huang, A. Lardeau, and Y. Aurégan, J. Appl. Phys. **117**, 124903 (2015).
[14]A. Santillán and S. I. Bozhevolnyi, Phys. Rev. B **84**, 064304 (2011).
[15]N. Jiménez, W. Huang, V. Romero-García, V. Pagneux, and J.-P. Groby, Appl. Phys. Lett. **109**, 121902 (2016).
[16]N. Jiménez, V. Romero-García, V. Pagneux, and J.-P. Groby, Phys. Rev. B **95**, 014205 (2016).
[17]N. Jiménez, V. Romero-García, V. Pagneux, and J.-P. Groby, Sci. Rep. **7**, 13595 (2017).
[18]I. S. Organization, *ISO 17497–2:2012 Acoustics—Sound-Scattering Properties of Surfaces—Part 2: Measurement of the Directional Diffusion Coefficient in a Free Field* (I. S. Organization, 2012).
[19]T. J. Cox and P. D'Antonio, *Acoustic Absorbers and Diffusers: Theory, Design and Application*, 3rd ed. (CRC Press, 2016).
[20]M. R. Stinson, J. Acoust. Soc. Am. **89**, 550 (1991).
[21]T. D. Rossing, F. Dunn, W. M. Hartmann, D. M. Campbell, and N. H. Fletcher, *Springer Handbook of Acoustics*, 1st ed. (Springer Publishing Company, Incorporated, 2007).
[22]ISO 17497-2:2012, *Acoustics—Sound-Scattering Properties of Surfaces—Part 2: Measurement of the Directional Diffusion Coefficient in a Free Field* (International Organization for Standardization, Geneva, Switzerland, 2012).
[23]L. Garcia-Raffi, L. Salmeron-Contreras, I. Herrero-Durá, R. Picó, J. Redondo, V. Sánchez-Morcillo, K. Staliunas, N. Adkins, A. Cebrecos, N. Jiménez *et al.*, Aerosp. Sci. Technol. **73**, 300 (2018).